JOURNAL OF Applied Polymer SCIENCE

Electrochemical Preparation and Characterization of Novel Polyethylene/Polyindene and Polystyrene/Polyindene Composites

Muzaffer Talu, Elif Uzluk, Bekir Sarı, Leyla Selam
Faculty of Science, Department of Chemistry, Gazi University, Teknikokullar, Ankara 06500, Turkey

Correspondence to: M. Talu (E-mail: mtalu@gazi.edu.tr)

ABSTRACT: In this study, the conducting homopolymer of indene and polyethylene/polyindene (PE/PIn) and polystyrene/polyindene (PS/PIn) composites have been electrochemically synthesized on platinum electrode in nonaqueous acetonitrile. The physical, electrochemical, thermal, and spectral properties of the synthesized PIn and their composites were investigated. The conductivities of PIn and the composites were measured with a four-probe technique. The conductivity of PIn was determined as 7.86×10^{-4} S/cm, whereas the conductivities of the PE/PIn and PS/PIn composites were determined to 6.42×10^{-5} S/cm and 5.64×10^{-5} S/cm, respectively. From Gouy scale magnetic susceptibility measurements, it was found that PIn and the composites had bipolaron natures. Fourier transform infrared spectra were taken to analyze the structural properties of PIn and the composites. The thermal properties of PIn and the PE/PIn and PS/PIn composites were investigated with thermogravimetric analysis, and it was found that they showed adequate thermal stability. According to the initial decomposition temperature among the composites, the composite including PE had the highest decomposition temperature with 450°C. The synthesized composites were different in aspect of morphology when compared to PIn. © 2012 Wiley Periodicals, Inc. J. Appl. Polym. Sci. 000: 000–000, 2012

KEYWORDS: composites; conducting polymers; electrochemistry; polyethylene; polystyrene

Received 11 September 2011; accepted 22 February 2012; published online
DOI: 10.1002/app.37586

INTRODUCTION

Electrically conducting polymers have been studied extensively because of their use in potential applications such as battery electrodes, corrosion protection, conducting textiles, gas separation membranes, light emitting diodes, electrochemical sensors, biosensors.[1–8] However, conducting polymers have poor mechanical and physical properties. These properties can be enhanced by forming composites from a conductive polymer and an insulating polymer.[9–11]

Polyindene (PIn) has also elicited much interest in recent years because of its high glass-transition temperature (T_g) and special optical properties.[12] PIn arises as an important optical polymeric material.[12] This is attributed to its "cyclic" structure that enables the phenyl ring present in the molecules to arrange in a horizontal fashion along the main polymeric chain, such that PIn exhibits a planar conformation.[12] In addition, oxidized indene polymer obtained with sulfuric acid offer variety of applications as dispersants, in dye and pigment preparations.[13] PIn derived by indene-coumarone reaction with sulfuric acid act as adhesives, printing inks, floor tiles, and friction tapes.[14] For example, PIn can be used for practical nanodevices, functional glass for sensing, optoelectronics, photocatalysis, and solar energy systems. Electrochemical and chemical oxidative methods have been adopted to synthesize granular, macrodimensioned particles, and one-dimensional of nanofibers of PIn.[15–20] PIn derived by indene-coumarone reaction with sulfuric acid act as adhesives, printing inks, floor tiles, and friction tapes.[19,20]

The aim of this study was to develop enhanced physical properties such as electrical and thermal stability and morphology of PIn using PE and PS insulating polymers. The electrochemically prepared PIn and the composites characterized by cyclic voltammetry (CV), FTIR, SEM, and X-ray diffraction analysis. The stability of PIn and the composites were investigated by thermogravimetric analysis. In this study, the electrochemically preparation and characterization of conducting composites of PIn, PE, and PS were investigated. There are limited articles in the literature about chemical preparation of PIn-based composite.[11] There have been no reports in the literature about the electrochemical synthesis and characterization of PE/PIn and PS/PIn composites.

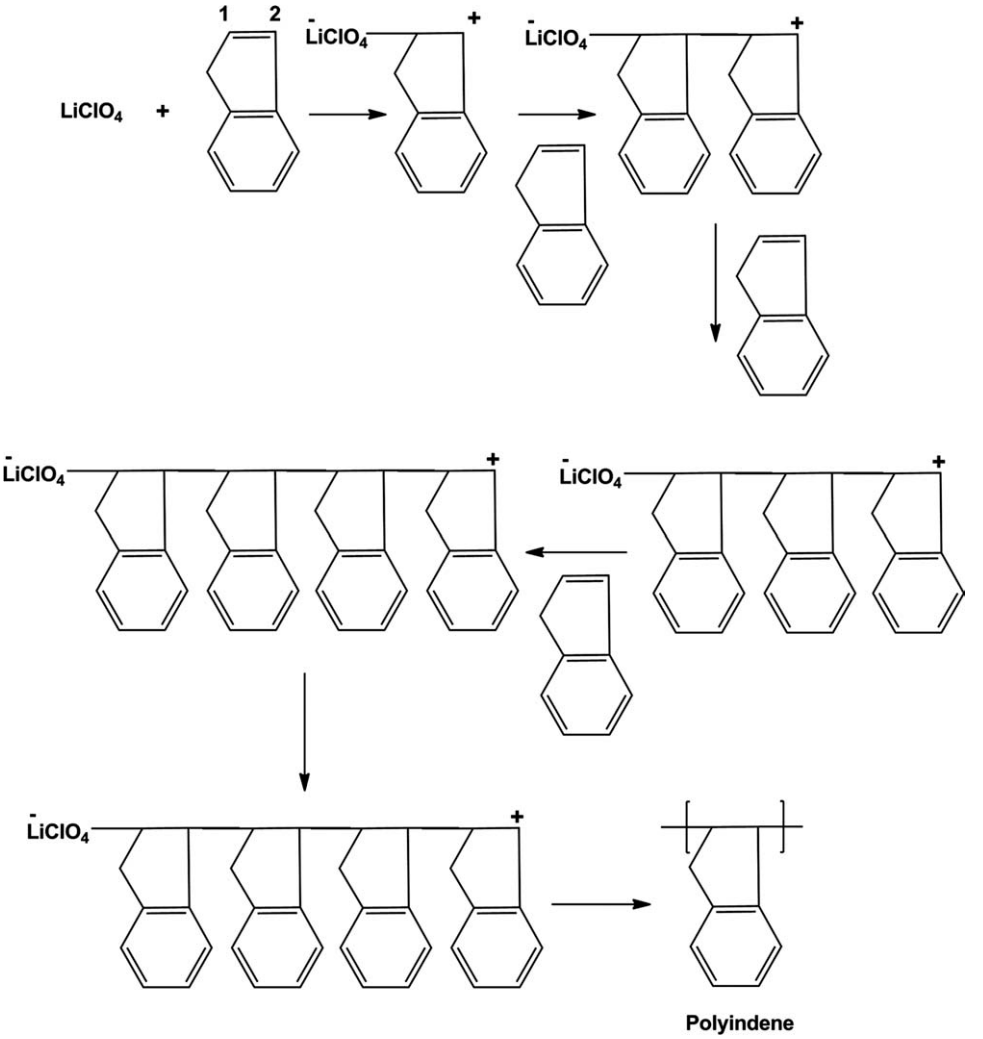

Scheme 1. Proposed polymerization for the formation of PIn.

EXPERIMENTAL

Materials

Indene (Aldrich, Germany) was freshly distilled under reduced pressure. Polystyrene = $\overline{M_w}$= 280,000 g, mp 93.0°C, n_D^{20} = 1.592 and polyethylene = high density, d (density) = 0.946 g/cm^3 were purchased from Merck, Germany. Lithium perchlorate ($LiClO_4$), acetonitrile, and chloroform (Aldrich, Germany) were used as received.

Synthesis of Polyindene

Polyindene (PIn) was synthesized over a platinum electrode surface using 0.1*M* indene and 0.3*M* $LiClO_4$ in an acetonitrile (70 mL) medium. The molar ratio of dopant anion to monomer was 3:1. Equal amounts of $LiClO_4$ were placed in both cell compartments. The cell was purged with nitrogen, and then acetonitrile and indene were introduced into the cell. Before the cyclic voltammetry was started, electrodes were placed, the solutions in each compartment of the cell were equilibrated and the cell was placed into a constant temperature bath. Their voltammograms were taken at a scan rate of 100 mV/s and were performed with repeating the potential sweeps between 0.00 V to +2.30 V by cyclic voltammetry. Maximum oxidation potential of indene was found 2.0 V at this process.[13] Electropolymerization was carried out at this potential for 18 h at 25°C and PIn was accumulated. Nitrogen gas was passed over the cell for 15 min. PIn-covered electrode was washed in acetonitrile and was dried in a vacuum oven at 75°C under 100 mbar pressure for 24 h. Then the brown colored PIn film was carefully removed from electrode surface as a solid state. The yield percentage of PIn was 35 wt %. The polymerization mechanism of PIn is given in Scheme 1.[11,17]

Preparation of the Polyethylene/Polyindene Composites

PE film was coated on the cleaned electrode surface from a 3 g/100 mL chloroform solution of PE.[21] The coating was carried out by dropping 1.0 mL of above solution onto each surface of the working electrode at 25°C. Equal amounts of $LiClO_4$ were placed in both cell compartments. The cell was purged with nitrogen, and then acetonitrile and indene were introduced into the cell. Before the cyclic voltammetry was started, PE-coated and other two electrodes were placed in electrolysis cell, the solutions in each compartment of the cell were equilibrated and the cell was placed into a constant temperature bath. PE-covered electrode

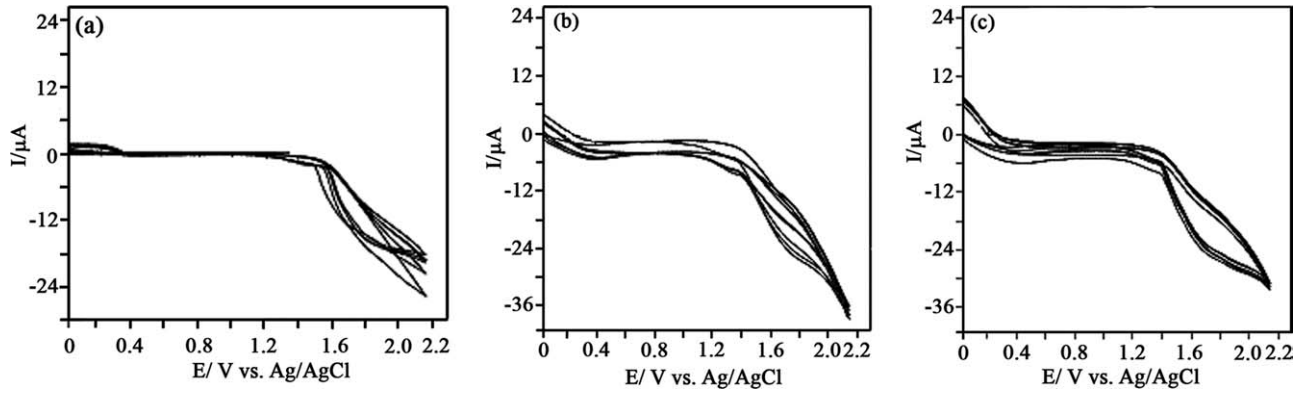

Figure 1. Cyclic voltammograms of (a) PIn, (b) PE/PIn composite, and (c) PS/PIn composite on Pt electrode in acetonitrile, scan rate = 0.1 V/s.

was dipped in a cell containing 0.1*M* indene and 0.3*M* $LiClO_4$ solution in acetonitrile (100 mL) medium and was covered with a second layer of PIn. The process was carried out in a constant duration of 18 h at 25°C. Nitrogen gas was passed over the cell for 15 min. The PE/PIn composites were washed in acetonitrile and were dried in a vacuum oven at 75°C under 100 mbar pressure for 24 h. Then the brown coloured PE/PIn films were carefully removed from electrode surface as a solid state.

Preparation of the Polystyrene/Polyindene Composites

PS was coated on the electrode surface from a 3 g/100 mL chloroform solution of PS at 25°C. Following a similar procedure in preparation of the polyethylene/polyindene (PE/PIn) composite. The brown coloured PS/PIn composite was obtained in by dropping-coating (D-C) method onto surface of platinum electrode.

Characterization

Electrochemical Measurements. Cyclic voltammetry of homopolymer and composites was performed with a PGS 2000D model potentiostat-galvonastat system at a scan rate of 100 mV/s, in a three-electrode cell with a platinum (Pt) wire as the counter electrode and an Ag/AgCl electrode as reference electrode. Pt wire electrode (2.5 cm^2) was used as working electrode. A nonaqueous Ag/AgCl electrode filled with acetonitrile containing 0.3*M* $LiClO_4$ saturated with AgCl was used as reference electrode. Electrodes mentioned above were carefully polished with abrasive paper (1500 mesh), and cleaned by acetone successively before each examination. It was used the same Pt electrode for keeping the constant surface conditions. Because the surface contamination greatly influences the rate of polymerization, the remaining polymer particles were completely removed by polishing with diamond paste. Acetonitrile was used as the solvent and $LiClO_4$ as the supporting electrolyte. All solutions were deaerated by a dry nitrogen stream and maintained at a slight nitrogen overpressure during experiments. Experiments were done at 25°C.

Infrared Spectroscopy. Fourier transform infrared (FTIR) spectra of the polymers were taken in KBr pellets with a Mattson-1000 model spectrometer (Ati Unicam, Cambridge, UK).

Thermal Analysis. Thermogravimetric analysis (TGA) of the polymer samples were recorded with DuPont 951 TGA model (Boston, MA) thermal analyzer under a nitrogen atmosphere up to 800°C at a heating rate of 10°C/ min.

Four-point Probe Technique. The conductivity of compressed pellets (4 ton/cm^2) of the homopolymer and composites was determined with the standard four-point probe technique at room temperature. The conductivity values of both the solution and electrode facing sides of the polymers were determined.

Gouy Balance. Magnetic susceptibility measurements were carried out with a Sherwood Scientific model MKI Gouy scale (UK). Finely powdered polymer samples were placed in a glass tube at a height of not less than 1.5 cm. This glass tube was placed into the hole of the magnetic balance, which was on a wooden bench, to obtain a constant value.

Scanning Electron Microscopy. Scanning electron microscopy (SEM) images of polymers were taken with JEOL JEM 100 CX II model instrument electron microscope (JEOL, Peabody, MA).

X-ray Diffraction Spectroscopy. Crystallization behaviors of the polymers were determined by D8-Advance-Bruker-AXS diffractometer employing CuKα ($\lambda = 0.15418$ nm) radiation over the range $5° \leq 2\theta \leq 50°$. Crystallinity degrees of (X_c) of the polymers were determined by area ratio method using the following equation:[22]

$$X_c = \frac{{}_0s^2 I_c(s) d}{{}_0s^2 I(s) d} \quad (1)$$

where s is the magnitude of the reciprocal-lattice vector which is given by $s = (2\sin\theta)/\lambda$ (θ is one-half the angle of derivation of the diffracted rays from the incident X-rays and λ is the wavelength); $I(s)$ and $I_c(s)$ are the intensities of coherent X-ray scatter from both crystalline and amorphous regions and from only crystalline region of polymer sample, respectively, and d is interplanar spacing.[22]

RESULTS AND DISCUSSION

Electrochemical Synthesis and Behavior

Controlled potential electrolysis (CPE) of indene was studied in acetonitrile on a Pt working electrode. Electrochemical behavior of PIn was studied by cyclic voltammetry (CV) $LiClO_4$-acetonitrile supporting electrolyte-solvent couple. Cyclic voltammogram of PIn is given in Figure 1(a). As seen in Figure 1(a), electropolymerization of indene starts with the formation of cation radical at 1.30 V. Main oxidation peak at 2.00 V versus Ag/AgCl

Table I. Yield, Conductivity, and Gout Balance Measurements of Polymers

Polymer	Medium	Supporting electrolyte	Yield (wt, %)	Conductivity (S/cm)	Magnetic susceptibility (μ_{eff}, BM)
PIn	Acetonitrile	$LiClO_4$	35	7.86×10^{-4}	−42
PE/PIn	Acetonitrile	$LiClO_4$	54	6.42×10^{-5}	−36
PS/PIn	Acetonitrile	$LiClO_4$	50	5.64×10^{-5}	−5

μ_{eff}, effective magnetic moment; BM, Bohr magneton.

for indene [Figure 1(a)]. These results were in agreement with literature.[15] The Pt surface is covered with PIn in the first scan. Indene is then oxidized on PIn-coated surface in the following scans. It was also observed such a decrease in the peak current during repetitive anodic scans. However, when the potential is held constant at the peak potential for few minutes and the scan is continued, a considerable increase in the peak current was observed indicating the conducting nature of the PIn film formed on the surface of the PIn-coated electrode. The oxidation steps (anodic peaks) were observed at 1.30 V and 2.00 V correspond to the oxidation of indene.

PE/PIn composite film was electrochemically prepared in two steps. In the first step, PE film was coated on the cleaned Pt electrode surface. In the second step, PE-covered electrode was dipped in a cell containing 0.1*M* indene and 0.3*M* $LiClO_4$ solution in acetonitrile medium. The multi-scan cyclic voltammograms taken for 0.1*M* indene and 0.3*M* $LiClO_4$ in acetonitrile on PE-covered electrode are shown in Figure 1(b). As seen in Figure 1(b), electropolymerization of indene starts with the formation of cation radical at 1.20 V. The third and fourth cycles were observed two oxidation waves at 1.20 and 2.14 V [Figure 1(b)]. These are the oxidation potentials of indene on the PE-coated electrode.

PS/PIn composite film was electrochemically prepared in two steps. In the first step, PS film was coated on the cleaned Pt electrode surface. In the second step, PS-covered electrode was dipped in a cell containing 0.1*M* indene and 0.3*M* $LiClO_4$ solution in acetonitrile medium. The cyclic voltammograms obtained for the oxidation of indene on PS-coated electrode are given in Figure 1(c). As seen in Figure 1(c), electropolymerization of indene starts with the formation of cation radical at 1.30 V. The third and fourth cycles were observed two oxidation waves at 1.30 and 2.05 V [Figure 1(c)]. These are the oxidation potentials of indene on the PS-coated electrode. The increase in the number of scans increases PIn deposition which in turn increases the current.

Polyethylene and polystyrene-coated electrode surface can be a porous structure; indene monomer diffuses through these pores to be oxidized on Pt surface. The indene radicals are bound to the active sites of polyethylene and polystyrene films and oxidized upon it after the pores are totally filled.[23] The voltammogram of the indene oxidation, which gives main oxidation peak at 2.14 and 2.05 V; these values are identical to those obtained for the indene oxidation on polyethylene and polystyrene-covered Pt electrode, respectively. Also main oxidation peak of indene is 2.00 V. This potential is agreement in with insulated polymer-coated platinum electrode results. According to these results, PIn, PE/PIn and PS/PIn composites are obtained.[23–25]

Polymerization Mechanism

The proposed polymerization mechanism for the formation of PIn is shown in Scheme 1. In case of PIn, electrophilic reaction of indene takes place in the presence of $LiClO_4$ thereby forming dimeric indanyl cation species. Combination with other indene units further propagates the molecular sequence and finally leads to the PIn chain. The chemistry that occurs between the cationic chain and $LiClO_4$ results in adhering of the ClO_4^- ion into the PIn chain at a localized bipolaron site, as a dopant.[11,17,20,26] The single terminal indanyl cation responsible for developing the PIn chain propagates in a planar fashion, causing the model PIn chain to breed in only one uniform direction with no side branch reactions. NMR spectra showed that the polymer chains were grown mainly via the coupling of the monomer at C(1), C(2) positions.[27]

Yield, Electrical Conductivity, and Magnetic Susceptibility

The yields, electrical conductivity, and magnetic susceptibility of the PIn homopolymer and PE/PIn and PS/PIn composites are summarized in Table I. The yields of PIn, PE/PIn, and PS/PIn are 35%, 54%, and 50% respectively.

As shown in Scheme 1, there were no conjugated bonds along the backbone of the PIn. It is known that conjugation is not enough to make a polymer material conductive. In addition, charge carriers in the form of extra electrons have to be injected or adsorbed into the material. Therefore, the conductivity value of PIn was determined to be lower than that of the other conjugated polymers.[11,17] As shown in Table I, the conductivity of PIn was found to be higher than of its composites. Among the homopolymer and composites, PIn had the highest conductivity with 7.86×10^{-4} S/ cm. The charge created on the doped PIn backbone (shown in Scheme 1) due to protonation in the form of bipolarons is responsible for EC in PIn. Goel et al.[19] measured that EC value of PIn is nearly 1.73×10^{-4} S/cm. It was also obtained similar conducting value of PIn homopolymer in this study. The conductivity value of the PIn homopolymer decreased with PE and PS into the composites. The conductivity values of PE/PIn and PS/PIn composites were 6.42×10^{-5} S/ cm and 5.64×10^{-5} S/cm, respectively. PE and PS affect the movement of the charges in the polymer. These results show that the conductivity of the composites is different that the conductivity of PIn. PIn and the composites were observed that the solution sides and the electrode sides of the films have some

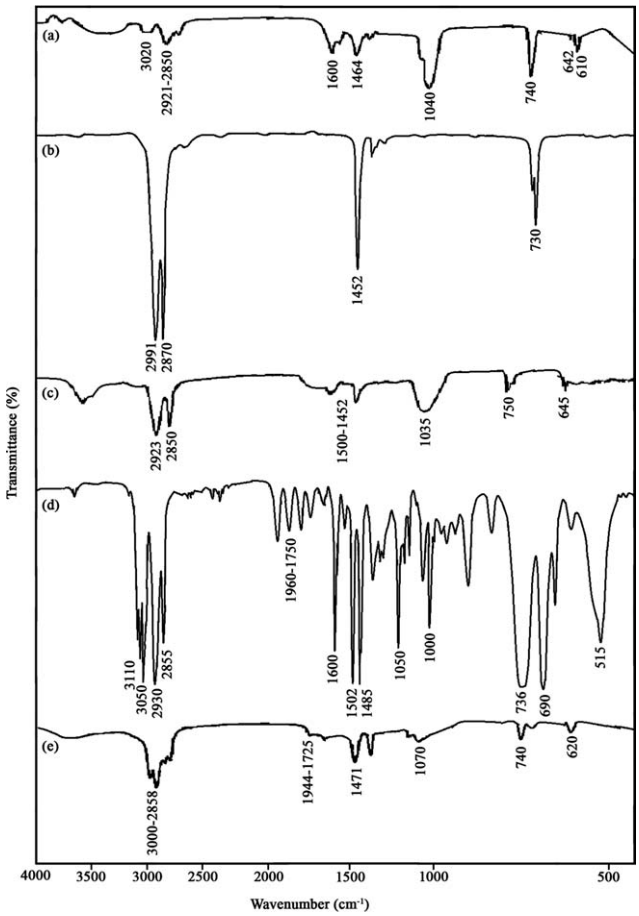

Figure 2. FTIR spectra of (a) PIn, (b) PE, (c) PE/PIn composite, (d) PS and (e) PS/PIn composite.

conductivity. This gives an idea about the homogeneity of the films, at least in terms of conductivity. Sarikaya et al.[18] determined that the conductivity values of PIn and the PIn/$CaCO_3$ conducting composites varied from 0.64×10^{-5} S/ cm to 2.11×10^{-5} S/cm. It was also obtained different and higher conducting value of composites in this study.

The magnetic properties of the composites have been considered by measuring the magnetic susceptibility. The magnetic susceptibility data of the polymers are also given in Table I. The values obtained from the Gouy measurements showed that the PIn homopolymer and the composites had diamagnetic properties, and their conducting mechanisms had a bipolaron nature.[9]

FTIR Results

FTIR spectrum in the spectral range 4000–500 cm^{-1} is used to characterize the structural organization of PIn, PE, PE/PIn, PS, and PS/PIn, as shown in Figure 2(a–e). FTIR spectra of PIn, PE, and PS shows different features compared with the composites.

As shown in the FTIR spectrum of electrochemically polymerized PIn [(Figure 2(a)], the aromatic C—H stretching band shifted to 3020 cm^{-1}, aliphatic C—H stretching band shifted to 2921–2850 cm^{-1}, the aromatic C=C stretching bands of indene, which is observed at 1640 cm^{-1}, has been shifted to 1600 cm^{-1}, the C—C ring stretching band belonging to C_1—C_2 atoms shifted to 1464 cm^{-1}, the C—H out-of-plane bands belonging to benzene shifted to 740–710 cm^{-1} in PIn's spectrum [Figure 2(a)], the band located at 610 cm^{-1} is attributed to the cis CH=CH bending vibration modes. C—H and C=C stretching bands are identical to PIn, which indicates that during the electropolymerization of PIn, aromatic ring was reserved and did not take part in the electropolymerization.[17,18] ClO_4^- groups generate the strong absorption peaks at 642 cm^{-1}. The FTIR results illustrate successful electropolymerization of PIn in doped state with sharp and well-resolved emergence of spectral bands. The FTIR spectrum of PIn exhibited the characteristic absorptions reported for PIn in the literature.[15–18,20,22]

The composites show all the bands of PIn and PE, PIn and PS, respectively. The FTIR spectrum of PE/PIn is given in Figure 2(c). The bands at aliphatic C—H symmetric and asymmetric stretching bands belonging to PE at 2923 cm^{-1} and 2850 cm^{-1} are observed. The aromatic C=C stretching band belonging to PIn and C—C stretching band belonging to PE shifted to 1500–1482 cm^{-1}, and the C—H out-of-plane bands belonging to PE and PIn shifted to 750 cm^{-1}. ClO_4^- groups generate the weak absorption peaks at 645 cm^{-1}.

The FTIR spectrum of PS/PIn composite [Figure 2(e)] at 3000–2858, 1944–1725, 1471, 1070, and 740 cm^{-1} were typical of aromatic C—H stretching vibration + aliphatic C—H stretching (for polyindene and polystyrene), and CH_2 asymmetric + symmetric stretching vibration, aromatic ring monosubstitution, C—C stretching band of the C_1—C_2 atoms + deformation CH_2, flexion C—H in the plane, and C—H out-of-plane bands, respectively. The intensity of C—H out-of-plane band has decreased. ClO_4^- groups generate the weak absorption peaks at 620 cm^{-1}. Thus, these were thought to proof of the composites. All bands shift slightly, which indicates that some interaction exists between PIn and insulating polymer.[18] C—C stretching is sharped and changed with PIn incorporation in the composites. These results indicate that the structure of polyindene backbone in PE/PIn and PS/PIn composites is different to that of PIn homopolymer.[11,17,18,28–32] These results support that the fact that PIn, PE/PIn and PS/PIn composites are successfully electrochemical synthesized.[24,25]

TGA Results

The decomposition temperatures of homopolymer and composites were determined by TGA. TGA curves of PIn, PE/PIn, and PS/PIn are shown in Figure 3(a–c). Thermal degradation temperature and residue % at 900°C obtained from these curves are shown in Table II. As shown in Table II, PE/PIn and PS/PIn composites showed one-step weight loss, whereas PIn decomposed in a two step. The first weight loss attributed to removal of dopant anions (ClO_4^-) and low-molecular weight oligomers from the polymer matrix, and the second weight loss step showed the decomposition of the polymer structure. The second decomposition occurs between 500 and 736°C, showing the degradation of polymer chain.

PIn shows two-step weight loss in the temperature range of 271–736°C [Figure 3(a)]. The weight loss is nearly 80%. However, the decomposition occurring at step one was due to

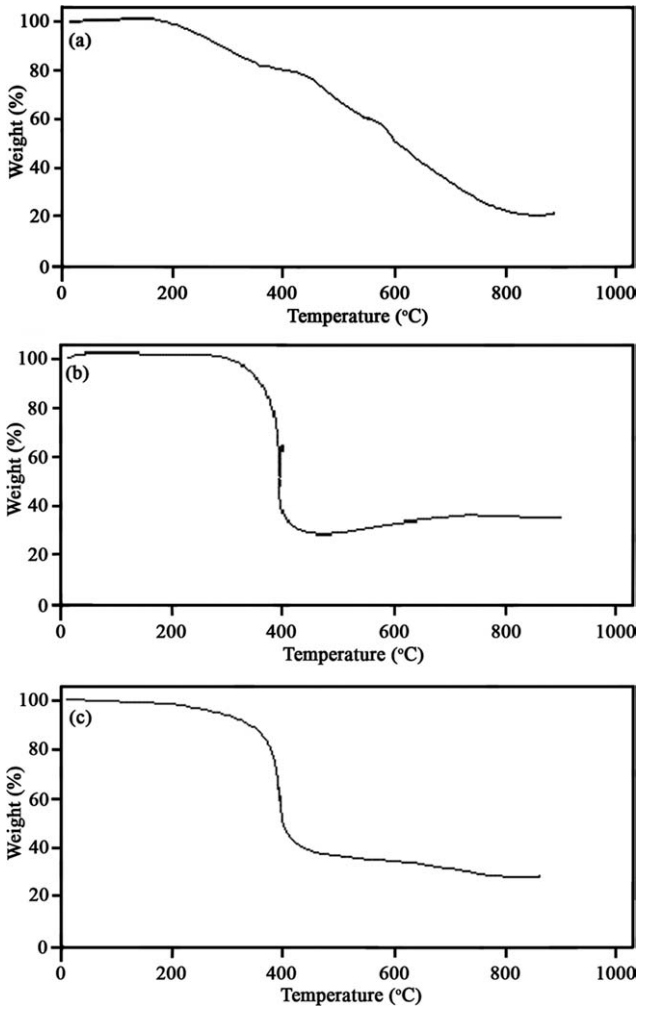

Figure 3. TGA curves of (a) PIn, (b) PE/PIn composite, and (c) PS/PIn composite.

degradation of the PE/PIn and PS/PIn chain structure. In decompositions in one step, the decomposition corresponds to both removal of dopant anions and degradation of polymer structure. A sharp weight loss appears in the temperature range 450–482°C for PE/PIn composite [Figure 3(b)] and 382–440°C for PS/PIn composite [Figure 3(c)]. The composites yields somewhat different patterns due to the presence of PE and PS. Thermal stability of the composites was investigated by measuring the initial decomposition temperatures, which were determined from first derivative of the TGA curves (Table II). The initial degradation temperatures are 405°C and 375°C for PE and PS, respectively.[33] When comparing to thermal stability of polymers, the initial degradation temperature is checked. The initial degradation temperatures are 270, 450, and 387°C for PIn, PE/Pin, and PS/PIn, respectively. Thus, the initial degradation temperatures of all the composites were observed to be higher than PIn.[17,32] As the presence of PE and PS was increased in the composite, the amount of residue left increased. The thermal stability of PIn increased with the prepared PE/PIn and PS/PIn composites. Among insulating polymers, PE increased thermal stability of pure polymers much more than PS. All composites are more thermally stable than the pure PIn, which can be explained by the fact that an interaction between PIn and insulating polymers restricts thermal motion of the PIn in the composites and enhances thermal stability of the composites.

In comparison to earlier reports[15,17–19] on thermal studies of PIn, here, PIn structure has shown to exhibit higher thermal stability characteristics, describing a thermal decomposition temperature range 500–736°C, in contrast to thermal decomposition temperature range 380–674°C. So, the thermal properties of PIn improved.[27,32]

SEM Results

The SEM micrographs of PIn and the composites are shown in Figure 4(a–c). The SEM micrograph of electrode side of PIn [Figure 4(a)] shows a granular structure.[17] When the morphologies of PIn and the composites (PE/PIn and PS/PIn) were compared, it was observed that the composites had quite different morphologies with PIn. PE/PIn showed a wafer-like structure [Figure 4(b)]. PS/PIn showed a closely porous structure [Figure 4(c)]. PE/PIn and PS/PIn composites look more compact than PIn.[9] Compared with the SEM micrograph (Figure 4) surface structure is changed. From these results, PIn insulating polymer-coated electrode surface to form a composite.[27,32]

XRD Results

Figure 5(a–c) shows the X-ray diffraction (XRD) patterns of PIn, PE/Pin, and PS/PIn composites. The values of crystalline and amorphous phase area and crystallinity (%) for PIn and the composites are presented in Table III. As seen from Figure 5(a–c), homopolymer and composites have different X-ray diffraction patterns from each other. Degree of crystallinity of PIn, PE/PIn, and PS/PIn were obtained as 14.6%, 40.8%, and 12.0%, respectively. XRD pattern of the PIn has broad and narrow peaks at $2\theta = 16°$, 18°, 22°, and 24°, respectively [Figure 5(a)]. The doped PE/PIn exhibits a higher degree of crystallinity that other doped PIn and PS/PIn [Figure 5(b)]. The X-ray diffraction profile of the PE/PIn has sharp peaks at $2\theta = 20°$, 24°, and 40°, respectively. It is seen that XRD peaks for PE/PIn composite are mostly different to those of PIn, indicating that the structure of PE was modified by PIn.[34] These results also indicate that PIn is semicrystalline in the composite, which suggests that the addition of PE improves the crystallization of the PIn molecular chains. It suggests also that an interaction exists at the interface of PIn and PE. From these results, PIn insulating polymer-coated electrode surface to form a composite.[32]

Table II. Thermal Decomposition Temperatures of Polymers

Polymer	T_i (°C)	T_m (°C)	T_f (°C)	Weight loss at 800°C
PIn	271	346	386	
	500	582	736	80
PE/PIn	450	473	482	70
PS/PIn	382	421	440	75

T_i, initial degradation temperature; T_m, maximum degradation temperature; T_f, final degradation temperature.

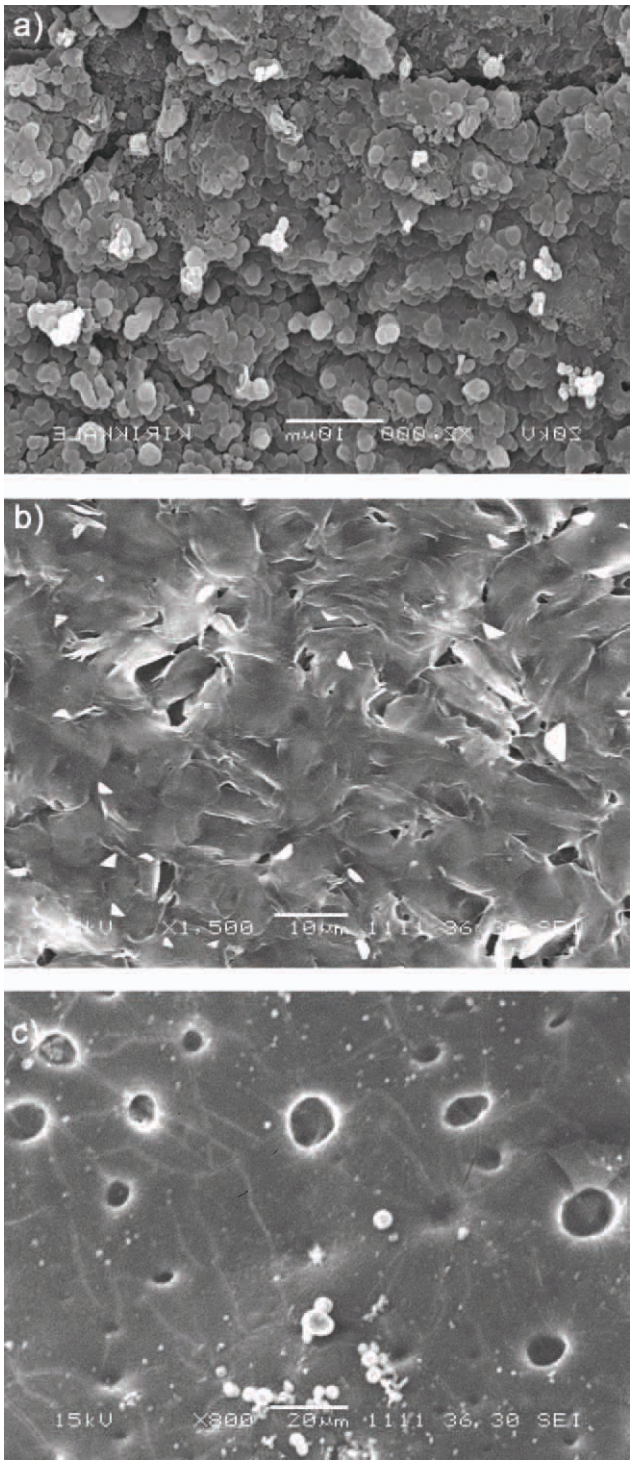

Figure 4. SEM migrograph of (a) PIn, electrode side, magnification ×2000, bar = 10 μm, (b) PE/PIn, electrode side, magnification ×1500, bar = 10 μm, and (c) PS/PIn, electrode side, magnification ×800, bar = 20 μm.

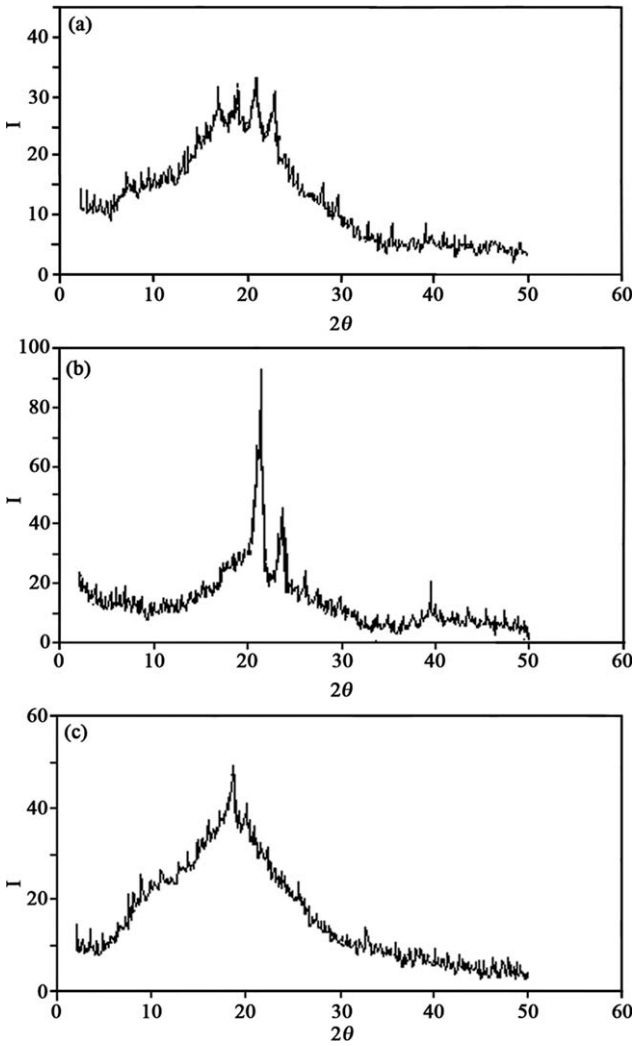

Figure 5. XDR patterns of (a) PIn, (b) PE/PIn composite, and (c) PS/PIn composite.

Table III. Crystallinity of Polymers

	Area		
Polymer	Cryst.	Amorph.	X_c (%)
PIn	14.4	86.4	14.6
PE/PIn	40.7	60.2	40.8
PS/PIn	12.2	88.3	12.0

CONCLUSIONS

In this study, PIn homopolymer was synthesized by electrochemical oxidation. It was modified the thermal and conductivity properties and morphology of PIn by electrochemically preparing PE/PIn and PS/PIn composites. The composites were found to be more thermally stable than that of PIn. These enhancements in thermal stability of the composites are ascribed to the interaction between host and guest materials. When it was compared conductivity changes with changing insulating polymers, it was observed some properties. PE and PS decreased the conductivity value of PIn. PIn and the composites showed different properties in the results of the FTIR and SEM analysis. The composites also showed different morphologies according

to the type of insulating polymer. PE/PIn and PS/PIn composites look more compact than PIn. It can be concluded that this work could also help in future studies devoted to rechargeable batteries, conducting films, sensors, and corrosion inhibitors.

ACKNOWLEDGMENTS

The authors gratefully thank the Gazi University Research Found (Project number: 05/2003-57) for financial support.

REFERENCES

1. Amanokura, J.; Suzuki, Y.; Imabayashi, S.; Watanabe, M. *J. Electrochem. Soc* **2001,** *148*, D43.
2. Le, H. N. T.; Garcia, B.; Deslouis, C.; Xuan, Q. L. *J. Appl. Electrochem.* **2002,** *32*, 105.
3. Kuhn, H. H.; Child, A. D.; Kimbrell, W. C. *Synth. Met.* **1995,** *71*, 2139.
4. Lin, C. W.; Hwang, B. J.; Lee, C. R. Mater. *Chem. Phys.* **1998,** *55*, 139.
5. Grenier, A.; Bolle, B.; Hesemann, P.; Obeski, J. M.; Sander, R. *Macromol. Chem. Phys.* **1996,** *197*, 113.
6. Lin, C. W.; Hwang, B. J.; Lee, C. R. *J. Appl. Polym. Sci.* **1999,** *73*, 2079.
7. Bhat, N. V.; Gadre, A. P.; Bambole, V. A. *J. Appl. Polym. Sci.* **2003,** *88*, 22.
8. Cosnier, S. Anal. *Bioanal. Chem.* **2003,** *377*, 507.
9. Gök, A.; Sari, B.; Talu, M. *J. Appl. Polym. Sci.* **2003,** *88*, 2924.
10. Migahed, M. D.; Ishra, M.; Fahmy, T.; Barakat, A. *J. Phys. Chem. Solids* **2004,** *65*, 1121.
11. Cabuk, T. Z.; Sari, B.; Unal, H. I. *J. Appl. Polym. Sci.* **2010,** *117*, 3659.
12. Kanaoka, S.; Ikeda, N.; Tanaka, A.; Yamaoka, H.; Higashimura, T. *J. Polym. Sci. Part A: Polym. Chem.* **2002,** *40*, 2449.
13. Beckmann, E.; Erren, S.; Baus, U.; Zimmermann, N.; Kromm, E.; Taeger, K.; Borschel, E.; Bury, W. U.S. Patent 5,753,775, **1998** (http://www.wikipatents.com/5753775.html).
14. Lewis, R. J. Hawley's Condensed Chemical Dictionary; Wiley: New York, **2002.**
15. Bozkurt, A.; Akbulut, U.; Toppare, L. *Synth. Met.* **1996,** *82*, 41.
16. Hahn, S. F.; Hillmyer, M. A. *Macromolecules* **2003,** *36*, 71.
17. Eristi, C.; Yavuz, M.; Yilmaz, H.; Sari, B.; Unal, H. I. *J. Macromol. Sci. A: Pure Appl. Chem.* **2007,** *44*, 759.
18. Sarikaya, S.; Yavuz, M.; Yilmaz, H.; Unal, H. I.; Sari, B. *Polym. Compos.* **2009,** *30*, 583.
19. Goel, S.; Mazumdar, N. A.; Gupta, A. *J. Polym. Res.* **2009,** *17*, 639.
20. Goel, S.; Mazumdar, N. A.; Gupta, A. *Appl. Surf. Sci.* **2010,** *256*, 4426.
21. Brandrup, J.; Immergut, E. H.; Grulke, E. A.; Abe, A.; Bloch, D. R. Polymer Handbook; Wiley: New York, **2005.**
22. Çimen, E. K.; Rzaev, Z. M. O.; Pişkin, E. *J. Appl. Polym. Sci.* **2005,** *95*, 573.
23. Kabasakaloglu, M.; Talu, M.; Yildirim, F.; Sari, B. *Appl. Surf. Sci.* **2003,** *218*, 84.
24. Sari, B.; Talu, M.; Yildirim, F.; Balci F. K. *Appl. Surf. Sci.* **2003,** *205*, 27.
25. Bonastre, J.; Lapuente, R.; Garces, P.; Cases, F. *Synth. Met.* **2009,** *159*, 1723.
26. Kennedy, J. P.; Midha, S.; Keszler, B. *Macromolecules* **1993,** *26*, 424.
27. Shurvell, H. F. In Handbook of Vibrational Spectroscopy, Vol.*3*; Chalmers, J. M.; Griffith, P. F., Eds.; Wiley: New York, **2002.**
28. Sari, B.; Talu, M.; Gok, A. *J. Appl. Polym. Sci.* **2003,** *87*, 1693.
29. Jerome, C.; Geskin, V.; Lazzaroni, R.; Bredas, J. L.; Thibaut, A.; Calberg, C.; Bodart, I.; Mertens, M.; Martinot, L.; Rogrigue, D.; Riga J.; Jerome, R. *Chem. Mater.* **2001,** *13*, 1656.
30. Jeoin, B. H.; Kim, S.; Choi, M. H.; Chung, I. J. *Synth. Met.* **1999,** *104*, 95.
31. Yavuz, A. G.; Uygun, A.; Bhethanabotla, V. R. *Carbohyd. Polym.* **2010,** *81*, 712.
32. Taylan, N. B.; Sari, B.; Unal, H. I. *J. Polym. Sci. Polym. Phys.* **2010,** *48*, 1290.
33. Tan, W. T.; Radhi, M. M.; Ab Rahman, M. Z.; Kassim, A. B. *J. Appl. Polym. Sci.* **2010,** *10*, 139.
34. Zanetti, M.; Lomakina, S.; Camino, G.; *Macromol. Mater. Eng.* **2000,** *279*, 1.